The *TRANSPORT INHIBITOR RESPONSE2* Gene Is Required for Auxin Synthesis and Diverse Aspects of Plant Development[1][C][W][OA]

Masashi Yamada[2], Katie Greenham[3], Michael J. Prigge[3], Philip J. Jensen[4], and Mark Estelle[3]*

Department of Biology, Indiana University, Bloomington, Indiana 47405

The plant hormone auxin plays an essential role in plant development. However, only a few auxin biosynthetic genes have been isolated and characterized. Here, we show that the *TRANSPORT INHIBITOR RESPONSE2* (*TIR2*) gene is required for many growth processes. Our studies indicate that the *tir2* mutant is hypersensitive to 5-methyl-tryptophan, an inhibitor of tryptophan synthesis. Further, treatment with the proposed auxin biosynthetic intermediate indole-3-pyruvic acid (IPA) and indole-3-acetic acid rescues the *tir2* short hypocotyl phenotype, suggesting that *tir2* may be affected in the IPA auxin biosynthetic pathway. Molecular characterization revealed that *TIR2* is identical to the *TAA1* gene encoding a tryptophan aminotransferase. We show that *TIR2* is regulated by temperature and is required for temperature-dependent hypocotyl elongation. Further, we find that expression of *TIR2* is induced on the lower side of a gravitropically responding root. We propose that *TIR2* contributes to a positive regulatory loop required for root gravitropism.

Auxin is known to play an important role in plant development (Davies, 1995). However, many aspects of auxin biology remain poorly understood. Auxin is synthesized primarily in young tissues, such as cotyledons, leaves, and roots (Ljung et al., 2001, 2005), and transported to other tissues where it is perceived by members of the TRANSPORT INHIBITOR RESPONSE1 (TIR1) auxin receptor family. Recent studies have dramatically increased our knowledge of auxin transport and signaling (Quint and Gray, 2006; Vieten et al., 2007). However, the pathways of auxin synthesis and their regulation are still relatively unclear.

Several indole-3-acetic acid (IAA) biosynthetic pathways have been proposed in plants based on research in plant-associated bacteria (Patten and Glick, 1996; Woodward and Bartel, 2005; Spaepen et al., 2007). There are two major types of pathways: the Trp-dependent and Trp-independent pathways. It has been hypothesized that plants have four Trp-dependent pathways that are generally named after an intermediate. In bacteria, the indole-3-pyruvic acid (IPA) pathway, one of the Trp-dependent pathways, has been described in detail (Koga, 1995; Spaepen et al., 2007). The current model for the IPA pathway involves a Trp aminotransferase oxidatively transaminating Trp to IPA. Subsequently, an IPA decarboxylase converts IPA to indole-3-acetaldehyde, and indole-3-acetaldehyde is oxidized to IAA. The IPA pathway is considered a major IAA biosynthetic pathway in plants, since potential intermediates have been isolated from different species (Sheldrake, 1973; Cooney and Nonhebel, 1991; Koga, 1995; Tam and Normanly, 1998). In addition, Trp transamination activity has been found in many plants (Gamborg, 1965; Forest and Wightman, 1972; Truelsen, 1973). Recently, two groups reported the identification of a gene called *TAA1*. This gene encodes an aminotransferase that converts Trp to IPA and functions in IAA biosynthesis (Stepanova et al., 2008; Tao et al., 2008).

To identify genes that are required for auxin synthesis, transport, and signaling, we previously screened for Arabidopsis (*Arabidopsis thaliana*) mutants that are resistant to auxin transport inhibitors, such as N-1-napthylpthalamic (NPA; Ruegger et al., 1997). The treatment of seedlings with NPA results in auxin accumulation in the root tip (Ljung et al., 2005). Thus, mutants that are resistant to NPA may have defects in synthesis, transport, or response because roots of these mutants are expected to have lower levels of IAA or reduced sensitivity to IAA. This screen succeeded in isolating mutations in seven genes with weak NPA-resistant phenotypes, including genes related to auxin signaling (*TIR1*), auxin transport (*TIR3*), and auxin

synthesis (*TIR7*; Ruegger et al., 1997, 1998; Ljung et al., 2005).

Here, we describe the characterization of *TIR2*, a gene whose function is required for auxin synthesis. Genetic and physiological analyses of the *tir2* mutant suggest that TIR2 is required for the Trp-dependent auxin synthesis pathway and functions as a Trp aminotransferase. Molecular cloning of *TIR2* reveals that the gene is identical to *TAA1* (Stepanova et al., 2008; Tao et al., 2008). We show that auxin regulates expression of *TIR2* in a tissue-specific manner. Furthermore, we show that *TIR2* is required for temperature-dependent hypocotyl elongation and that high temperature positively regulates expression of the *TIR2* gene, suggesting that temperature regulates hypocotyl elongation directly by stimulating auxin synthesis. Finally, we provide evidence that *TIR2* functions in a positive regulatory loop required for root gravitropism.

RESULTS

The *tir2* Mutant Exhibits an Altered Response to NPA But Not Auxin

The *tir2-1* mutant was isolated in a screen for seedlings that are resistant to the growth inhibiting properties of NPA. The mutant displays an NPA-resistant phenotype similar to other *tir* mutants, such as *tir1* and *tir3* (Ruegger et al., 1997). When grown on 5 μM NPA, wild-type seedlings exhibited approximately 60% root elongation after 3 d compared to untreated controls, while *tir2-1* seedlings displayed 75% root elongation (Fig. 1A). In addition to root inhibition, NPA treatment induced elongation of root hairs in wild-type (Columbia-0 [Col-0]) roots (Fig. 1, E and F). In *tir2-1* plants, this response was clearly reduced (Fig. 1, G and H). Furthermore, wild-type roots produced additional columella cells after treatment with NPA due to auxin accumulation in the root tip (Fig. 1, I and J), while *tir2-1* roots had fewer columella cells even after treatment with NPA (Fig. 1, K and L). These results suggest that the roots of the *tir2* mutants either have lower levels of auxin or are less sensitive to auxin.

To understand whether *TIR2* is involved in auxin transport, *tir2-1* mutant seedlings were treated with the synthetic auxins 2,4-dichlorophenoxyacetic acid (2,4-D) and 1-naphthaleneacetic acid (NAA) as well as the natural auxin IAA. It is known that auxin influx carriers promote uptake of 2,4-D but not NAA (Delbarre et al., 1996), while NAA but not 2,4-D are substrates of the efflux carriers. Thus, the auxin influx transporter mutant (*aux1-7*; Marchant et al., 1999) is resistant to 2,4-D but not NAA (Fig. 1, C and D). In contrast, the auxin efflux transporter mutant (*pin2/agr1*; Chen et al., 1998; Luschnig et al., 1998; Muller et al., 1998) is hypersensitive to NAA because the hormone accumulates within the cells of mutant plants (Fig. 1D). If the *tir2* mutants are deficient in

auxin influx or efflux, we expect that they will be either resistant or hypersensitive to 2,4-D and NAA, respectively. In Figure 1, B to D, we show that *tir2-1* seedlings display the same response as *Col-0* to all three auxins tested. In contrast, *aux1-7* was less sensitive to all concentrations of IAA tested (Fig. 1B). This suggests that *tir2-1* can transport auxin effectively. Furthermore, these data indicate that the *tir2-1* mutants respond normally to the auxin signal, unlike *tir1-1* (Ruegger et al., 1998; Dharmasiri et al., 2005; Fig. 1, B–D). As a control, we tested the *tir7-1* mutant, an allele of the *ANTHRANILATE SYNTHASE ALPHA SUBUNIT1* (*ASA1*) gene. This mutant has lower levels of IAA (Ljung et al., 2005). Figure 1, B to D, shows that *tir2-1* and *tir7-1* have similar responses to the three auxins tested. These data suggest that the *TIR2* gene is not involved in auxin transport or signaling but in auxin synthesis.

TIR2 Is Required for Diverse Auxin-Dependent Processes in the Seedling

In addition to the NPA-resistant phenotype, the *tir2* mutants display many auxin-related defects. Figure 1, E to H, shows that mutant seedlings produce shorter root hairs than the wild type. In addition, the mutant has fewer lateral roots, a reduction in root gravitropism (Fig. 2, A and B), and defects in vascular tissue in cotyledons (data not shown). The diversity of these defects suggests that *TIR2*-dependent auxin synthesis contributes to many aspects of plant growth.

Increased temperature has a dramatic effect on Arabidopsis seedling growth. Wild-type seedlings grown at 29°C have higher levels of IAA and as a consequence longer hypocotyls, petioles, and roots, compared to seedlings grown at 22°C (Fig. 2, C and D; Gray et al., 1998). In contrast, the hypocotyls and petioles of *tir2-1* seedlings are only slightly longer at the higher temperature, indicating that *TIR2* is required for this response.

Our data show that *tir2* is not resistant to exogenous auxin. However, if the mutant is deficient in IAA synthesis, we expect to see changes in the level of auxin-regulated transcription, particularly at sites of auxin production, such as young leaves, cotyledons, and root tips (Ljung et al., 2001, 2005). To address this question, we crossed the *DR5rev:GFP* auxin-responsive reporter into the *tir2-1* mutant (Benková et al., 2003). The GFP signal was slightly weaker in hypocotyls, petioles, cotyledons, and root tips of *tir2-1* compared to *Col-0* at 22°C (Fig. 3, A, C, E, and G). At 29°C, the GFP signal increased markedly in the root tips and shoots of wild-type seedlings (Fig. 3, B and F). Furthermore, in wild-type roots the meristem cells were larger at the higher temperature (Fig. 3, E and F, arrow). In *tir2-1* seedlings, the GFP signal increased only slightly at 29°C, and the meristem cells were smaller than in wild-type plants (Fig. 3, E–H, arrow). Although the level of *DR5rev:GFP* activity was affected in *tir2-1*, the distribution of signal was similar to *Col-0*,

Figure 1. *tir2-1* seedlings are resistant to NPA but not auxin. A, Root elongation on 5 μM NPA. B to D, Root elongation on medium containing IAA (B), 2,4-D (C), and NAA (D). E to H, Root hairs after treatment with 5 μM NPA. Seven-day-old seedlings were grown on ATS medium for 3 d before transfer to medium containing NPA. Bar = 300 μm. I to L, *Col-0* and *tir2-1* seedlings stained with Lugol stain. Four-day-old seedlings were transferred to medium with or without NPA and stained after 9 d. Bar = 50 μm. [See online article for color version of this figure.]
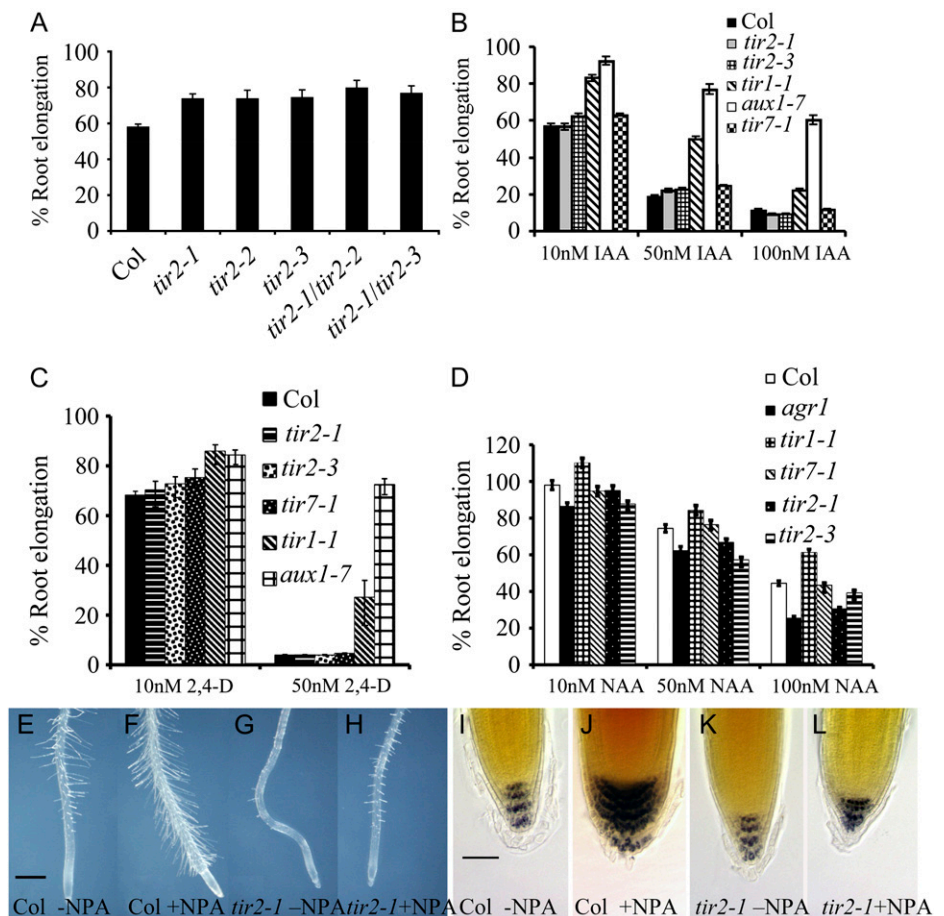
suggesting that *tir2-1* is deficient in auxin synthesis but not transport.

We also examined *DR5rev:GFP* activity in *tir2-1* after NPA treatment. In wild-type plants, *DR5rev:GFP* activity increased in the root tips after treatment with NPA due to accumulation of auxin (Fig. 3, I and J). However, NPA treatment did not significantly alter GFP signal in the mutant (Fig. 3, K and L). These data also suggest that the *TIR2* gene is required for auxin synthesis.

The *TIR2* Gene Is a Trp Aminotransferase

To determine the function of *TIR2*, we isolated the gene using a positional cloning approach. *TIR2* was mapped to an interval on chromosome one that included 30 genes (Supplemental Fig. S1A). The sequence of these genes was determined in the *tir2-1* allele, and a mutation was found in the third exon of *At1g70560* encoding an alliinase-like protein. The mutation results in the substitution of a Glu at Gly-171. Recently, this gene has been described as *TRYPTOPHAN AMINOTRANSFERASE OF ARABIDOPSIS1* (*TAA1*; Stepanova et al., 2008; Tao et al., 2008). To confirm that *tir2-1* is an allele of *TAA1*, two T-DNA insertion lines (*tir2-2/wei8-3* SALK_127890 and *tir2-3/wei8-4* SALK_022743; Alonso et al., 2003; Stepanova

et al., 2008) were obtained and analyzed. Both T-DNA insertion lines shared similar defects with *tir2-1*, including NPA resistance (Fig. 1A), shorter root hairs, and shorter hypocotyls and petioles at 29°C (data not shown). Complementation analysis indicated that *tir2-2* and *tir2-3* are alleles of *tir2-1* (Fig. 1A). Further, the *TAA1* cDNA under control of the *Cauliflower mosaic virus 35S* promoter was introduced into *tir2* mutant plants. These lines displayed a wild-type phenotype, including normal NPA response (Supplemental Fig. S2A) and seedling morphology (data not shown), confirming that *TIR2* is the same gene as *TAA1*.

The amino acid sequence of TIR2 is similar to that of garlic (*Allium sativum*) alliinase (Supplemental Fig. S1B). The function of alliinase has previously been characterized in garlic and onion (*Allium cepa*; Kuettner et al., 2002). This enzyme catalyzes the conversion of a specific nonprotein sulfur-containing amino acid called alliin to allicin, a compound with antibiotic activity. To understand how TIR2 is related to alliinase-like proteins in other plant species, we performed a phylogenetic study using available sequences from land plants. These proteins fell into two major clades (Supplemental Fig. S3). The garlic and onion alliinases together with a number of uncharacterized proteins define one clade, while TIR2/TAA1 is in the second clade together with two additional Arabidopsis pro-
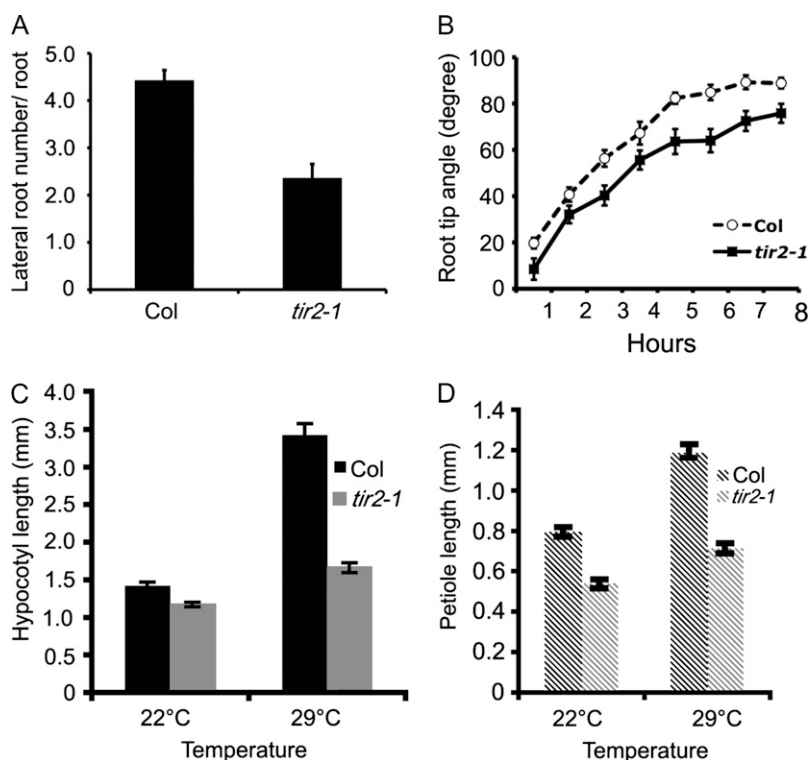
Figure 2. Auxin-related defects in the *tir2* mutant. A, Number of lateral roots on 10-d-old *Col-0* and *tir2-1* plants. B, Gravity response of *Col-0* and *tir2-1* roots. Seedlings were grown in a vertical orientation for 7 d and reoriented at time 0. C and D, Response of hypocotyls (C) and petioles (D) to increased temperature.

teins and proteins from diverse species, including the moss *Physcomitrella patens*. Stepanova et al. (2008) have named the two additional Arabidopsis proteins TAR1 and TAR2 and present evidence indicating that these proteins also function in IAA biosynthesis. Our data show that TIR2/TAA1 and the TAR1/2 proteins are in a separate lineage from garlic and onion alliinase (Supplemental Fig. S3). Further, structural studies show that the garlic alliinase is very similar to aminotransferases (Kuettner et al., 2002). Together with the earlier studies of Stepanova et al. (2008) and Tao et al. (2008), our analysis indicates that TIR2 is a Trp aminotransferase that synthesizes IPA from Trp (Fig. 4A).

The *TIR2* Gene Is Required for Auxin Synthesis

To further explore the possibility that TIR2 functions in the IPA pathway, we examined the sensitivity of the *tir2* mutant to 5-methyl Trp (5-MT), a Trp analog that inhibits Trp synthesis (Hull et al., 2000). If Trp is a substrate of TIR2, the *tir2* mutant should be hypersensitive to 5-MT. The data in Figure 4B show that this is the case. As controls, *tir1-1*, *pin2*, *aux1-7*, and *tir7-1* mutants were also treated with 5-MT. All of these mutants were more sensitive to 5-MT than wild-type plants (Fig. 4B). However, for *tir1*, *pin2*, and *aux1*, the difference was quite small. In contrast, *tir7-1*, deficient in Trp synthesis, was even more sensitive than *tir2* (Ljung et al., 2005). It has already been shown that the double mutants of the cytochrome P450s (*cyp79b2 cyp79b3*) are hypersensitive to 5-MT (Zhao et al., 2002). These two genes function in the IAOx pathway,

one of the Trp-dependent pathways. Overexpression of *TIR2* rescued the 5-MT-sensitive phenotypes of the *tir2* mutants (Supplemental Fig. S2B).

If the *TIR2* gene encodes a Trp aminotransferase, it may be possible to rescue some aspects of the mutant phenotype by providing additional IAA or IPA. Indeed, exogenous IAA or IPA dramatically increased *tir2-1* hypocotyl length at high temperature (Fig. 4, C and D) consistent with the proposed function of TIR2.

The *TIR2* Gene Is Expressed at Sites of Auxin Production

Auxin is produced at high levels in young developing leaves and cotyledons and at lower but still significant levels in roots (Ljung et al., 2001, 2005). To determine if *TIR2* is expressed in these tissues, we generated *TIR2* transcriptional GUS fusion lines using 3.4 kb of sequence upstream of the *TIR2* ATG. GUS expression was detected in young leaves and cotyledons as well as the vascular tissue in shoots, hypocotyls, and roots (Fig. 5, A–C). However, GUS staining was not detected in the root meristem.

To extend these results, we generated a translational fusion of the *TIR2* cDNA with *GUS* under control of the *TIR2* promoter and introduced it into the *tir2-1* mutant. This construct restored the wild-type phenotype to the mutant, indicating that the fusion protein is functional (Supplemental Fig. S4, A–C). The pattern of expression was similar to that of the transcriptional fusion except that GUS staining was more restricted in cotyledons and young leaves. Strong staining was found in the tips of young leaves and the margins of

Figure 3. *DR5rev:GFP* expression responds to high temperature and NPA treatment. A to H, *DR5rev:GFP* expression in hypocotyls and petioles (A–D) and roots (E–H) after growth at 22°C for 7 d (A, E, C, and G) or for 4 d at 22°C and 3 d at 29°C (B, F, D, and H). Bars = 200 μm in A to D and 50 μm in E to H. Arrows indicate larger cells (E and F) in the root meristem of the wild type at 29°C and smaller cells (G and H) in the root meristem of *tir2-1* at 29°C. I to L, *DR5rev:GFP* expression in 7-d-old seedlings 4 d after treatment with 5 μM NPA. Bar = 30 μm.
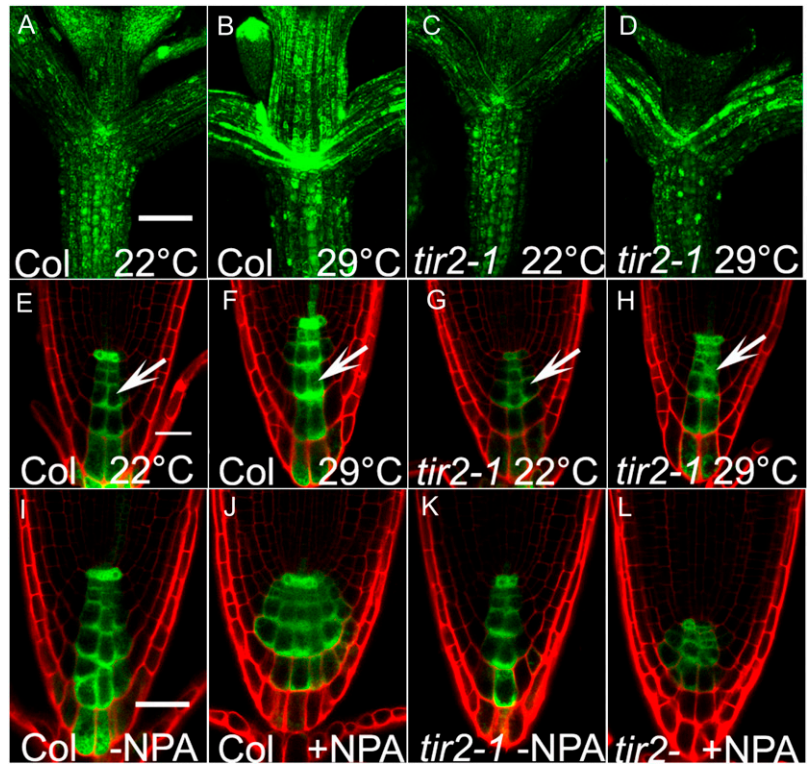
cotyledons (Fig. 5, D–H). Like the transcriptional fusions, we did not observe staining in the columella or distal meristem. However, a band of strong staining was detected in the proximal meristem. At this point, it is not known why this staining was not observed in the transcriptional fusion line. One possibility is that regulatory sequences are contained within the *TIR2* coding region. Stepanova et al. (2008), using a *TAA1:TAA1-GFP* fusion line, observed the strongest GFP signal in the quiescent center (QC) of etiolated seedlings. Although the significance of these differences is not clear, we note that the transgene we used for our studies was able to complement the mutant phenotype.

Auxin Regulates Expression of the *TIR2* Gene

The temporal and spatial distribution of IAA plays an important role in plant development. The concen-

Figure 4. The function of TIR2 in IAA biosynthesis. A, Schematic diagram of the IPA pathway. B, Root elongation after treatment with 5-MT. C and D, Hypocotyl length in seedlings grown on IPA (C) and IAA (D). Seedlings were grown at 22°C for 3 d followed by 4 d in the absence or presence of compound at 29°C. The effect of IPA and IAA on hypocotyl length is expressed as a percentage increase compared to medium without compound.
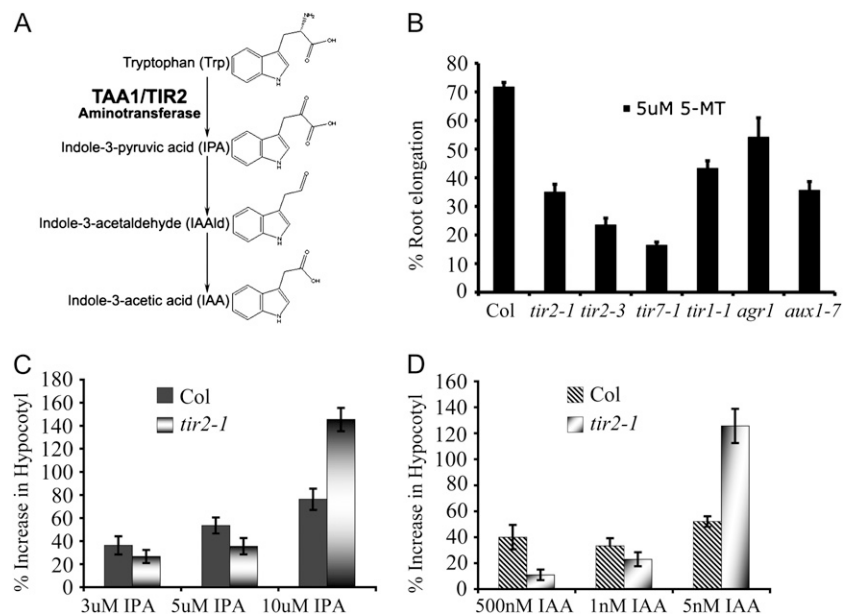
Figure 5. Analysis of *TIR2* expression in *pTIR2*:*GUS* and *pTIR2*:*TIR2-GUS* lines. GUS staining in *pTIR2*:*GUS* (A–C) and *pTIR2*:*TIR2-GUS tir2-1* (D–H) seedlings. Bars = 1 mm in A, 125 μm in B, C, F, and G, 500 μm in D, 250 μm in E, and 50 μm in H. Eight-day-old seedlings (A), 6-d-old seedlings (B and C), and 9-d-old seedlings (D–H) are shown.

tration of IAA in specific tissues is regulated by changes in auxin synthesis and transport. Although the regulation of IAA synthesis is poorly understood, recent studies have shown that IAA synthesis is regulated by other plant hormones, such as ethylene (Stepanova et al., 2005). In addition, there is evidence that feedback inhibition of IAA biosynthesis contributes to the control of IAA levels (Ljung et al., 2001, 2005). To determine if *TIR2* may be part of this feedback mechanism, we examined the effect of auxin treatment on expression of the *TIR2:TIR2-GUS* transgene. The data in Figure 6A show that GUS staining in the cotyledons is reduced after IAA treatment. However, because GUS is a stable enzyme, GUS staining is not a sensitive indicator of decreased transcription of the reporter gene. Consequently, we measured *TIR2* RNA levels in the hypocotyls and cotyledons of auxin-treated *Col-0* seedlings using quantitative reverse transcription (RT)-PCR. The results show that *TIR2* levels decreased substantially within 2 h of auxin treatment (Fig. 6B). Even after 8 h, *TIR2* levels have not recovered

to the level of untreated seedlings. These results suggest that IAA negatively regulates *TIR2* transcription.

In contrast to the cotyledon, we see a dramatic enhancement in GUS staining in the root tips of auxin-treated *pTIR2:TIR2-GUS* plants (Fig. 6C). At this point, it is not clear if this regulation is transcriptional or posttranscriptional.

Previously, it has been reported that treatment with 1-aminocyclopropane-1-carboxylic acid (ACC) (the precursor of ethylene) induces expression of genes related to auxin synthesis (Stepanova et al., 2005, 2008; Růzicka et al., 2007). Since auxin is known to induce ethylene biosynthesis, it is possible that the effect of auxin on *TIR2* expression requires ethylene. To determine if this is the case, we treated *pTIR2:GUS* and *pTIR2:TIR2-GUS* seedlings with IAA together with aminoethoxyvinylglycine (AVG; an inhibitor of the ethylene biosynthetic enzyme; Amrhein and Wenker, 1979; Lieberman, 1979). ACC treatment increased GUS staining in *DR5:GUS* lines in the root meristem as described previously (Stepanova et al., 2005; Růzicka et al., 2007; Supplemental Fig. S5). Also consistent with earlier studies, treatment with 10 μM 5-MT or 10 μM ACC plus 5-MT did not induce *DR5:GUS* expression, suggesting that ethylene induces *DR5:GUS* expression in roots by regulating genes in auxin synthesis (Supplemental Fig. S5). In contrast, the addition of AVG did not affect IAA-regulated changes in either the transcriptional or translational fusion lines, suggesting that auxin affects *TIR2* expression independently of ethylene (Supplemental Fig. S5).

The phenotype of the *tir2* mutant indicates that TIR2-dependent auxin synthesis is required for a normal gravitropic response. Since curvature in the root is dependent on an asymmetry in auxin levels across the root, we wondered if this asymmetry results in differential *TIR2* expression on the upper and lower side of the root. To investigate this, we grew *pTIR2:TIR2-GUS* seedlings in the vertical orientation, turned them 90°, and stained for GUS after 8 h. The results in Figure 6, D and E, show that GUS staining increased in the epidermal cells on the lower side of the root but decreased in the epidermis on the upper side of the root, consistent with preferential auxin transport. Treatment with NPA abolished the gravitropic response and resulted in symmetrical high-level expression of *TIR2-GUS*, confirming that the gravity response of *TIR2* is related to asymmetric auxin transport (Fig. 6F). These results suggest that a positive feedback loop contributes to increased auxin synthesis on the lower side of the root, thus amplifying the gravitropic response.

High Temperature Induces Expression of the *TIR2* Gene

In Arabidopsis seedlings, elevated temperature results in an increase in auxin levels. This increase stimulates both hypocotyl and petiole length as well as an increase in cell size in the root meristem (Gray et al., 1998). Because *tir2* seedlings do not respond to

Figure 6. Regulation of *TIR2* by auxin. A, GUS staining of *pTIR2*:*TIR2-GUS* seedlings at intervals after treatment with 10 μM IAA. B, Relative *TIR2* RNA levels in aerial plant parts after treatment with 50 μM IAA measured by quantitative RT-PCR. *TIR2* levels at time 0 were set to 100%. Values are the mean of eight determinations from three independent RNA preparations. Error bars represent SD. C, GUS staining of *pTIR2*:*TIR2-GUS* seedlings after treatment with 10 μM IAA for 3, 6, and 12 h. D to F, GUS staining of *pTIR2*:*TIR2-GUS* before (D) and 8 h after 90° rotation (E and F). Seedling in F was treated with 50 μM NPA.
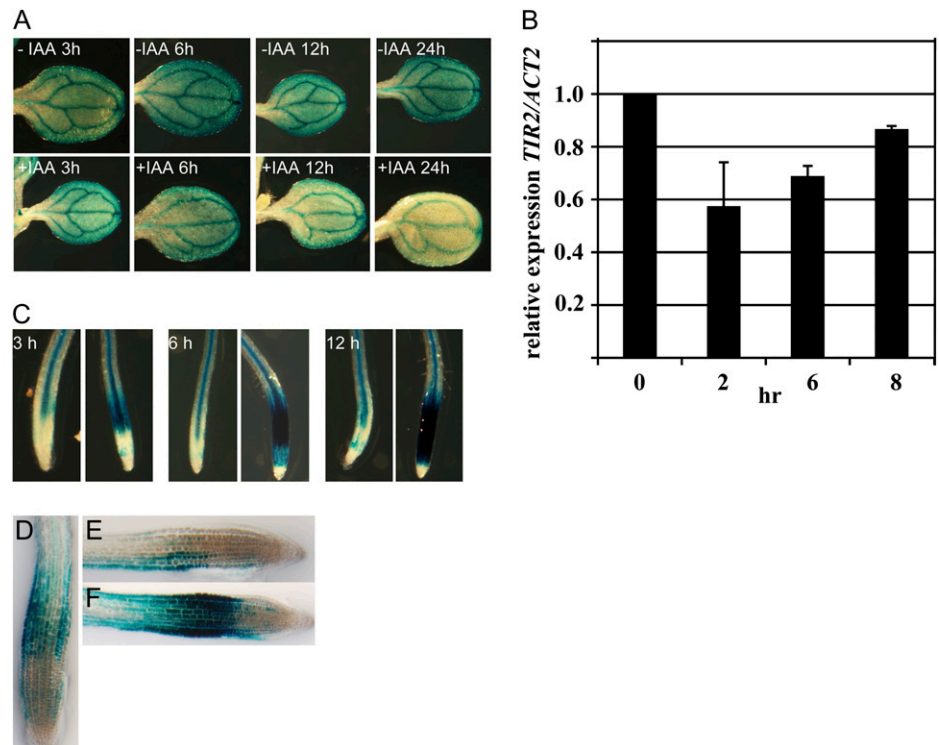
increased temperature, we reasoned that regulation of *TIR2* may be important for the temperature effect on auxin levels. To investigate this, we examined GUS levels in *pTIR2*:*TIR2-GUS* and *pTIR2*:*GUS* lines at 22°C and 29°C. The data in Figure 7 show that GUS levels increase in the cotyledon, hypocotyls, and root in response to the higher temperature, indicating that *TIR2* transcription is regulated by high temperature. Since we have already shown that expression of *TIR2* is decreased in much of the seedling in response to auxin, the effect of high temperature is probably independent of auxin signaling.

The *TIR2* Gene Is Required for Root Meristem Development

So far we have shown that *TIR2* is required for hypocotyl and petiole elongation, lateral root formation, gravitropism, and root hair formation. To learn more about the biological function of *TIR2*, we generated a *tir2-1 tir7-1* double mutant. The double mutant had a much more severe phenotype than the respective single mutants. The root lengths of the *tir2-1* and *tir7-1* single mutants were similar to the wild type, while the *tir2-1 tir7-1* double mutants formed short roots with very diverse phenotypes (Fig. 8, A and B). The more robust seedlings displayed a 60% reduction in root length compared to the wild type. More severely affected seedlings formed extremely short roots. Neither the *tir2-1* or *tir7-1* single mutants had an obvious root meristem defect, whereas the *tir2-1 tir7-1* double mutant had a clear defect (Fig. 8, C–E). To identify

which cells are disrupted in the root tips, these double mutants were crossed with a QC25 enhancer-trap line, which expresses the *GUS* gene in all QC cells (Sabatini et al., 2003). QC cells were detected in these lines by GUS staining, and columella cells were visualized with Lugol staining. In wild-type roots, two QC cells and four layers of columella cells were observed as expected (Fig. 8C). However, in the roots of weakly affected double mutant plants, only one QC cell was detected and the columella was disrupted (Fig. 8D). In severely affected seedlings, QC and columella cells were not observed (Fig. 8E). In addition, the total number of cells in the root meristem decreased in the *tir2-1 tir7-1* double mutant compared with the wild type, the *tir2-1* mutant, and the *tir7-1* mutant (data not shown).

To examine the distribution of auxin in the mutant lines, we crossed in the *DR5*:*GFP* construct. A slight decrease in GFP signal was observed in the single mutants (Fig. 8, G and H). However, in the double mutants, GFP signal was either decreased (Fig. 8I) or absent (Fig. 8J) in the root tips. Surprisingly, GFP was still detected in the vascular tissue of double mutant roots (Fig. 8J; Supplemental Fig. S6). This suggests that genes related to *TIR2*, such as *TAR1* and *TAR2*, or a different auxin biosynthetic pathway may be more important for auxin synthesis in these tissues.

DISCUSSION

Recent studies confirm that auxin synthesis occurs through multiple pathways in Arabidopsis, including
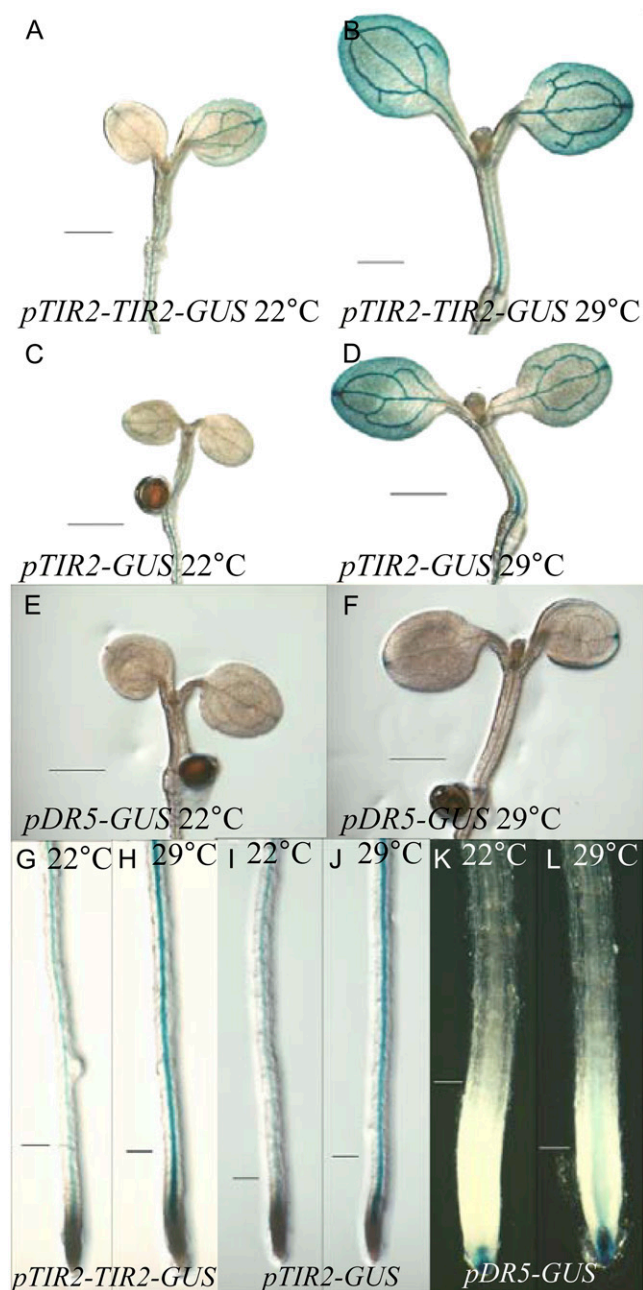
Figure 7. Effect of temperature on *TIR2* expression. GUS staining in 4-d-old seedlings in *pTIR2:TIR2-GUS*, *pTIR2:GUS*, and *DR5:GUS* lines at 22°C (4 d at 22°C) and at 29°C (2 d at 22°C, 2 d at 29°C). A, B, G, and H, *pTIR2:TIR2-GUS*. C, D, I, and J, *pTIR2:GUS*. E, F, K, and L, *DR5:GUS*. A, C, E, G, I, and K, 22°C. B, D, F, H, J, and L, 29°C. Bars = 1 mm in A to F, 250 μm in G to J, and 125 μm in K and L.

the TAM pathway and the IPA pathway (Cheng et al., 2006; Stepanova et al., 2008; Tao et al., 2008). Although the pathways may be partially redundant, their precise role in various aspects of plant development remains to be fully explored. Here, we show that *TIR2/TAA1*, encoding a Trp aminotransferase, is required for diverse processes in the seedling, including temperature-

dependent hypocotyl elongation and root gravitropism. Our results extend previous studies that demonstrate a role for *TIR2/TAA1* in a variety of growth processes during seedling development, including temperature-dependent hypocotyl growth, root gravitropism, root hair formation, and lateral root development.

TIR2 Is Required for the IPA Pathway

Early studies suggested that the IPA pathway is a major source of IAA in plants (Koga, 1995; Spaepen et al., 2007). However, until recently the enzymes in the pathway were unknown. The *tir2-1* mutant was recovered in a screen for NPA resistance that identified genes in diverse aspects of auxin biology, including auxin perception (*TIR1*), response (*TIR5/ARF7*), transport (*TIR3*), and synthesis (*TIR7/ASA1*; Harper et al., 2000; Gil et al., 2001; Dharmasiri et al., 2005; Kepinski and Leyser, 2005; Ljung et al., 2005). Typically, the behavior of NPA-resistant mutants on various auxins provides useful information on the function of the gene product. The *tir2-1* mutant responds normally to IAA, 2,4-D, and 1-NAA, suggesting that it is not deficient in auxin response or transport. In contrast, hypersensitivity to 5-MT is consistent with a defect in Trp-dependent IAA synthesis via the IPA pathway. The fact that *tir2-1* is rescued by exogenous IPA and IAA also strongly supports this hypothesis.

The *TIR2* gene encodes an alliinase-like protein structurally related to aminotansferases. Recently, two groups reported the identification of a Trp aminotransferase named TAA1 and demonstrated a role for this protein in auxin synthesis (Stepanova et al., 2008; Tao et al., 2008). We have confirmed that *TIR2* is identical to *TAA1*. In the *tir2-1* allele, Gly-171 is changed to Glu. This residue is conserved among all members of the alliinase/transaminase family and is part of the so-called strained loop involved in pyridoxal phosphate cofactor binding (Kuettner et al., 2002). It is likely that substitution of Glu at this position would disrupt this structure and pyridoxal phosphate binding.

TIR2 Regulation

In bacteria, the IPA decarboxylase is the rate-limiting step in IAA synthesis (Spaepen et al., 2007). Our results suggest that this may be the case in plants as well. Overexpression of *TIR2* did not result in growth defects, such as those observed when *YUCCA* is overexpressed (Zhao et al., 2001). Further, *35S:TIR2* lines displayed normal sensitivity to exogenous Trp, suggesting that increasing endogenous IPA levels does not result in the synthesis of more IAA (Supplemental Fig. S2C). Based on these results, it seems likely that IPA decarboxylase is limiting for auxin biosynthesis, at least under our conditions. The characterization of this enzyme in plants will address this question in the future.

Figure 8. Phenotype of the *tir2-1 tir7-1* double mutants. A, Root length of 7-d-old seedlings. B, Eight-day-old *tir2-1 tir7-1* seedlings. C to E, Expression of QC25 (blue) and Lugol staining (dark blue) in *Col-0* (C) and *tir2-1 tir7-1* (D and E) seedlings. Bar = 50 μm for the 8-d-old seedlings (C–E). F to J, Expression of *DR5rev:GFP* (green) in *Col-0* (F), *tir2-1* (G), *tir7-1* (H), and *tir2-1 tir7-1* (I and J). Propidium iodide staining (red). Bar = 50 μm for the 5-d-old seedlings (F–J).
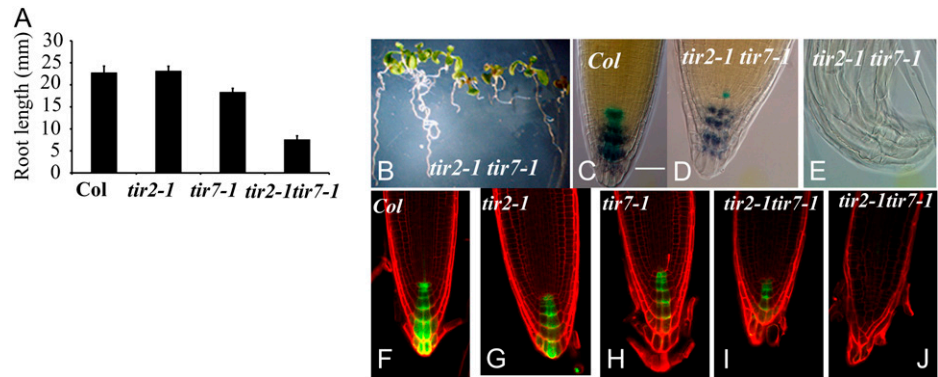
Although TIR2/TAA1 does not appear to be limiting, our results indicate that *TIR2* is highly regulated during development. Localized changes in auxin level are known to play a key role in embryogenesis, meristem establishment and maintenance, organogenesis, and tropic growth. The role of auxin transport during these processes is well established, but information on the role of auxin synthesis in the regulation of auxin flux is just beginning to emerge (Cheng et al., 2006; Stepanova et al., 2008; Tao et al., 2008). Expression of the *TIR2/TAA1* gene is spatially restricted during embryo development, and seedling development is consistent with existing models (this study; Stepanova et al., 2008; Tao et al., 2008).

In addition, we show that *TIR2* promoter activity is dramatically regulated in the seedling in response to auxin, indicating that auxin synthesis is subject to feedback regulation. In the aerial part of the seedling, *TIR2* expression is significantly reduced upon auxin treatment. This mechanism may play an important role in the precise regulation of auxin levels during growth processes. In a previous study, Tao et al. (2008) demonstrated that *TAA1* expression is reduced in the hypocotyl in response to shade despite the fact that auxin levels increase and hypocotyl elongation is stimulated in shade conditions. These authors also show that most of the auxin in a shade-responding seedling is synthesized in the cotyledons and leaves and is transported into the hypocotyl. Based on our results, we propose that this auxin represses transcription of *TIR2* in the hypocotyl.

In previous studies, we showed that Arabidopsis seedlings grown at elevated temperature have higher levels of IAA and that this change results in increased hypocotyl elongation (Gray et al., 1998). The *tir2* mutants are deficient in temperature-dependent growth stimulation, suggesting that the IPA pathway may be regulated by temperature. Indeed, we find that transcription of *TIR2* is strongly increased at 29°C compared to 22°C. Thus, it seems likely that the temperature effect is at least partly due to increased flux through the IPA pathway. Since TIR2/TAA1 is not limiting, we expect that the IPA decarboxylase is also regulated by temperature. In the future, it will be interesting to determine what other environmental conditions regulate the IPA pathway.

TIR2 and Root Growth

Our results indicate that *TIR2* is expressed in a narrow band in the proximal root meristem. Further, *TIR2* expression in this region is auxin sensitive, suggesting the existence of a positive regulatory loop that may have an important function during root growth. The structure and function of the root meristem is regulated by an auxin gradient with a maximum at the QC. This gradient is established through the action of members of the PIN family of auxin efflux carriers and maintained by an auxin transport loop that cycles auxin from the QC through the columella to the epidermal layer and back to the QC via the provascular tissue (Blilou et al., 2005; Grieneisen et al., 2007; Scheres, 2007). By itself, the *tir2-1* mutation does not confer an obvious defect in meristem structure. However, the phenotype of the *tir7-1 tir2-1* double mutant clearly indicates that *TIR2* functions in meristem maintenance. The *tir7-1* mutation affects ASA1 function and therefore acts upstream of TIR2/TAA1. Because both ASA1 and TIR2/IAA1 function redundantly with other members of their respective families, we infer that the combination of both mutations results in a further reduction in IAA levels in the root tip. We propose that auxin synthesized in the proximal meristem through the IPA pathway contributes to the auxin transport loop. Auxin regulation of *TIR2*, and perhaps other genes in the pathway, would facilitate stringent regulation of the auxin maximum. Consistent with this, double mutants that are deficient in both TAA1 and TAR2 have a similar meristem defect as the *tir2 tir7* mutants, indicating that TAR2 also contributes to this pathway (Stepanova et al., 2008).

It is important to note that the pattern of *TIR2* expression we observe with the *TIR2:TIR2-GUS* line differs slightly from that observed by Stepanova et al. (2008) using a whole gene GFP fusion. In that study, the highest level of GFP signal was observed in the QC, whereas we don't observe any GUS staining in the QC. In addition, cell-type specific array data indicate that *TAA1* is broadly expressed in the root, with the highest level in the stele (Birnbaum et al., 2003; Petersson et al., 2009). At this point, the reasons for these differences are not clear. However, we note that

the *TIR2:TIR2-GUS* transgene rescues the *tir2* mutant phenotype, indicating that TAA1 function is not required in the QC.

TIR2 also has an important role in root gravitropism. During gravitropic growth, auxin is preferentially transported from the columella into the epidermal cell layer on the lower side of the root, resulting in decreased growth of these cells relative to the cells on the upper side. Our results show that root curvature is associated with increased *TIR2* expression in the lower epidermal cells and concomitant loss of expression on the upper side. These changes would have the effect of increasing the asymmetry in auxin concentration and thus amplify the growth response.

Several recent studies have shown that parameters related to auxin transport are sufficient to model the formation and maintenance of the auxin maximum in the root meristem (Blilou et al., 2005; Kramer et al., 2008). Our study, together with other recent studies, suggests that regulation of auxin synthesis may also be an important factor in meristem behavior.

MATERIALS AND METHODS

Plant Material, Growth Conditions, and Treatments

All mutants and transgenic lines used in this study were in the *Col-0* ecotype. The T-DNA insertion lines *tir2-2* (SALK_127890) and *tir2-3* (SALK_022743) were obtained from the Arabidopsis Biological Resource Center at Ohio State University. Seeds were surface sterilized in 30% commercial bleach and 0.02% Triton X-100 and plated on ATS media [1% Suc, 5 mM KNO_3, 2.5 mM KH_2PO_4, pH 5.6, 2 mM $MgSO_4$, 2 mM $Ca(NO_3)_2$, 50 μM $CuSO_4$, 1 μM $ZnSO_4$, 0.2 μM $NaMoO_4$, 10 μM NaCl, and 0.01 μM $CoCl_2$; Lincoln et al., 1990] containing 7 g agar in 1 L. Seedlings were grown at 21°C to 23°C under continuous light conditions in square petri dishes.

Assay for Root Gravitropism

Root gravitropic response was assayed in a manner similar to the method of Lincoln et al. (1990). Four-day-old seedlings were transferred to new ATS plates and held in an incubator in a vertical orientation for 1 to 2 h. The plates were then rotated 90°, and at 1-h intervals the plates were removed from the incubator and the root tip angles were measured. Each point represents at least 10 seedlings.

Map-Based Cloning

The *tir2-1* mutant in *Col-0* was crossed to Landsberg *erecta*. NPA-resistant plants were selected from F2 populations based on root length and root hair phenotypes. DNA was isolated by cetyl-trimethyl-ammonium bromide from these F2 plants. NPA-resistant phenotypes were confirmed in the F3 generation.

For rough mapping, *TIR2* was placed in an interval between markers *F4N2* (110.4 centimorgans) and nga11 (115.55 centimorgans) on chromosome one. After fine mapping, *TIR2* was mapped between base pair 31246 of BAC F24J13 and base pair 35655 of BAC F15H11. The primers for mapping were designed using information from the CEREON collection (http://www.Arabidopsis.org/).

Assays for Root, Hypocotyl, and Petiole Elongation

To perform root elongation assays, 3- or 4-d-old seedlings were grown on ATS plates and transferred to ATS plates containing 5 μM NPA, 5 μM 5-MT, and other compounds. Root length was measured 3 or 4 d after transfer. For hypocotyl elongation assays, seedlings were grown on an ATS plate for 2 to approximately 3 d at 22°C, transferred to new plates, and grown at either 22°C or 29°C and incubated for 4 d. Lengths of roots, hypocotyls, and petioles were measured using a Nikon SMZ1500 dissecting scope and Image SXM software (http://www.liv.ac.uk/~sdb/ImageSXM/).

Plant Vectors and Transformations

The *TIR2* cDNA with or without stop codons and the *TIR2* promoter were cloned using Gateway cloning technology (Invitrogen) and recombined into *pMDC32* and *pMDC163* (Curtis and Grossniklaus, 2003). For *35S-TIR2*, *TIR2* cDNA was amplified from cDNAs generated by RT-PCR SuperScript II (Invitrogen) from total RNA from *Col-0* seedlings, cloned to *pENTR/D-TOPO* (Invitrogen), and recombined into *pMDC32* containing a *35S* promoter. Primers used for *35S-TIR2* were *pENTR TIR2* forward (5′-CACCATGGT-GAAACTGGAGAACTCG-3′) and *TIR2* reverse (5′-CTAAAGGTCAATG CTTTTAATGAG-3′). For *pTIR2:GUS*, a 3.4-kb region from the start codon of the *TIR2* gene was amplified from BAC F24J13 using primers *pENTR TIR2* promoter forward (5′-CACCTGAAGATGCTCTTACTTAAATTTA-3′) and *TIR2* promoter reverse (5′-CTTCTTCTTCTTGGTTTGGTC-3′), cloned, and recombined into pMDC163. For *pTIR2:TIR2-GUS*, the *TIR2* promoter including 90 bp from the ATG and the *TIR2* cDNA without stop codon were cloned and digested by *Xho*I and *Asc*I (New England Biolabs). The digested fragment of the *TIR2* cDNA without the stop codon was ligated into the digested *TIR2* promoter in *pENTR/D-TOPO* and recombined into *pMDC 163*. Primers used for the *TIR2* promoter with 90 bp of the first exon were *pENTR TIR2* promoter forward and *TIR2* promoter-cDNA reverse (5′-TGATCCAGATTGACCAC-GAAA-3′). Primers used for the *TIR2* cDNA without the stop codon were *pENTR TIR2* forward and *TIR2* no stop reverse (5′-AAGGTCAATGCTTT-TAATGAGC-3′).

Microscopy and Confocal Microscopy

For assays for root and hypocotyl elongation, images were collected using a dissecting microscope (Nikon SMZ1500) with a digital camera (Nikon DMX 1200). For detecting QC cells and columella cells, roots were observed by a Nikon E800 microscope. For detecting GFP signals, seedlings were observed under a Leica TCS SP confocal microscope. Seedlings were mounted in a 0.1 mg/mL propidium iodide (10 mg/mL; Sigma-Aldrich P-4170).

Staining

Seedlings were stained in GUS staining solution in 0.5 mg/mL 5-bromo-4-chloro-3-indolyl-β-glucuronic acid in *N,N*-dimethylformamide, 0.5 M sodium phosphate buffer (pH 7.2), 10% Triton X-100, 100 mM potassium ferrocyanide, and 100 mM potassium ferricyanide for 15 to approximately 18 h at 37°C. The orientation of seedlings after gravitropism was marked by removing one cotyledon prior to GUS staining. For Lugol staining, seedlings were stained in Lugol solution (Sigma-Aldrich L-6146) for 1 to approximately 3 h at room temperature.

Treatment of pTIR2:TIR2-GUS, pTIR2:GUS, and DR5:GUS Lines

Six-day-old seedlings were grown on ATS plates and transferred to ATS media on the six-well cell culture plate (Corning) containing 10 μM IAA, 10 μM IAA AVG, 10 μM AVG, 10 μM 5-MT, 10 μM ACC, 10 μM ACC 5-MT, and 10 μM IAA ACC. Seedlings were grown for 2 d under continuous white light at room temperature. To examine the effects of temperature, seedlings were grown on ATS at 22°C for 2 d before transfer to 29°C. Two days later, seedlings were stained for GUS.

Quantitative RT-PCR Analysis

To examine *TIR2* expression in response to auxin, total RNA was isolated from the aerial parts of 6-d-old seedlings 2, 6, and 8 h after treatment with 50 μM IAA using Tri-reagent (Sigma-Aldrich). Three micrograms of total RNA were used in reverse transcription reactions using SuperScript III reverse transcriptase (Invitrogen) and 20-mer oligo(dT) primer. Real-time quantitative PCR was performed using the LightCycler 480 Instrument (Roche Diagnostics) with LightCycler 480 Probes Master and Universal ProbeLibrary. Quantification of the *TIR2* RNA levels was performed using LightCycler software relative to expression of *ACTIN2*. Primers were designed using the Universal ProbeLibrary Assay Design Center (https://www.roche-appliedscience.com/

sis/rtpcr/upl/adc.jsp; Roche Applied Science). Primers were as follows: tir2f, 5′-GCCGCTCCTTTTTACTCCA-3′; tir2r, 5′-TGTACATACCCGACCGAACA-3′; Actin2f, 5′-CCGCTCTTTCTTTCCAAGC-3′; and Actin2r, 5′-CCGGTAC-CATTGTCACACAC-3′. The data represent the average fold change in *TIR2* transcript levels 2, 6, and 8 h after 50 μM IAA treatment, compared to seedlings treated with Murashige and Skoog alone.

Phylogenetic Analysis

Most protein sequences were extracted from data sets derived from genome sequencing projects: Arabidopsis (*Arabidopsis thaliana*; The Arabidopsis Information Resource version 8; http://www.arabidopsis.org), *Populus trichocarpa* (Poptr1_1.Jamboreemodels, http://genome.jgi-psf.org/Poptr1_1), *Ricinus comunus* (TIGRcastorWGSr0.1, http://castorbean.jcvi.org/), *Vitis vinifera* (Vitis_vinifera_peptide_v1, http://www.genoscope.cns.fr/spip/Vitis-vinifera-e.html), *Medicago truncatula* (20080227_imgag_protMAPPED_NO_OVERLAP, http://www.medicago.org/), *Oryza sativa* (TIGRv5.0, http://rice.plantbiology.msu.edu/), *Zea mays* (AZM5, http://maize.jcvi.org/), *Sorghum bicolor* (Sorbi1_Genemodels_Sbi1_4_aa, http://genome.jgi-psf.org/Sorbi1), *Selaginella moellendorffii* (Selmo1_Genemodels_Filteredmodels2_aa, http://genome.jgi-psf.org/Selmo1), and *Physcomitrella patens* (Phypa1_1.Filteredmodels3, http://genome.jgi-psf.org//Phypa1_1). Additional sequences were identified in The Institute for Genomic Research Transcript Assemblies from *Aquilegia formosa* × *pubescens*, *Pinus taeda*, *Picea glauca*, *Ceratopteris richardii*, and *Marchantia polymorpha* (http://plantta.jcvi.org/). The remaining sequences were identified in the GenBank Nonredundant protein and High Throughput Genomic Sequence databases. *Physcomitrella*, *Selaginella*, and *Populus* gene models were manually adjusted from the genomic sequences based on homology, splicing predictions, and EST data. The sequences were aligned using *T-COFFEE* (Notredame et al., 2000) and adjusted using *MACCLADE* (Maddison and Maddison, 2003). For Bayesian inference, the analysis was run with four runs of four chains for 3,000,000 generations using *MRBAYES 3.1.2* with the parameters aamodelpr = mixed, nst = 6, and rates = invgamma on the Indiana University BigRed computing cluster (Huelsenbeck and Ronquist, 2001). Maximum parsimony bootstrap support values were generated using the same protein alignment and *PAUP** beta10 for Mac (Swofford, 1998).

Supplemental Data

The following materials are available in the online version of this article.

Supplemental Figure S1. Positional cloning of the *TIR2* gene.

Supplemental Figure S2. Assay for root elongation of *p35S:TIR2* lines.

Supplemental Figure S3. TAA1/TIR2-related proteins in plants.

Supplemental Figure S4. The *pTIR2:TIR2-GUS* gene rescues the *tir2* mutant.

Supplemental Figure S5. GUS staining in *pTIR2:TIR2-GUS* and *DR5:GUS* seedlings.

Supplemental Figure S6. Expression of *DR5rev:GFP* in the *tir2-1 tir7-1* double mutant.

LITERATURE CITED

Alonso JM, Stepanova AN, Leisse TJ, Kim CJ, Chen H, Shinn P, Stevenson DK, Zimmerman J, Barajas P, Cheuk R, et al (2003) Genome-wide insertional mutagenesis of *Arabidopsis thaliana*. Science **301**: 653–657

Amrhein N, Wenker D (1979) Novel inhibitors of ethylene production in higher plants. Plant Cell Physiol **20**: 1635–1642

Benková EE, Michniewicz MM, Sauer MM, Teichmann TT, Seifertová DD, Jürgens GG, Friml JJ (2003) Local, efflux-dependent auxin gradients as a common module for plant organ formation. Cell **115**: 591–602

Birnbaum K, Shasha DE, Wang JY, Jung JW, Lambert GM, Galbraith DW, Benfey PN (2003) A gene expression map of the Arabidopsis root. Science **302**: 1956–1960

Blilou I, Xu J, Wildwater M, Willemsen V, Paponov I, Friml J, Heidstra R,

Aida M, Palme K, Scheres B (2005) The PIN auxin efflux facilitator network controls growth and patterning in Arabidopsis roots. Nature **433**: 39–44

Chen R, Hilson P, Sedbrook J, Rosen E, Caspar T, Masson PH (1998) The *Arabidopsis thaliana* AGRAVITROPIC 1 gene encodes a component of the polar-auxin-transport efflux carrier. Proc Natl Acad Sci USA **95**: 15112–15117

Cheng Y, Dai X, Zhao Y (2006) Auxin biosynthesis by the YUCCA flavin monooxygenases controls the formation of floral organs and vascular tissues in Arabidopsis. Genes Dev **20**: 1790–1799

Cooney T, Nonhebel H (1991) Biosynthesis of indole-3-acetic acid in tomato shoots: measurement, mass-spectral identification and incorporation of ^{2}H from ^{2}H$_2$O into indole-3-acetic acid, d- and l-tryptophan, indole-3-pyruvate and tryptamine. Planta **184**: 368–376

Curtis MD, Grossniklaus U (2003) A gateway cloning vector set for high-throughput functional analysis of genes in planta. Plant Physiol **133**: 462–469

Davies PJ (1995) Plant Hormones: Physiology, Biochemistry, and Molecular Biology. Kluwer Academic, Dordrecht, The Netherlands

Delbarre A, Muller P, Imhoff V, Guern J (1996) Comparison of mechanisms controlling uptake and accumulation of 2,4-dichlorophenoxy acetic acid, naphthalene-1-acetic acid, and indole-3-acetic acid in suspension-cultured tobacco cells. Planta **198**: 532–541

Dharmasiri N, Dharmasiri S, Estelle M (2005) The F-box protein TIR1 is an auxin receptor. Nature **435**: 441–445

Forest JC, Wightman F (1972) Amino acid metabolism in plants. III. Purification and some properties of a multispecific aminotransferase isolated from bushbean seedlings (*Phaseolus vulgaris* L.). Can J Biochem **50**: 813–829

Gamborg OL (1965) Transamination in plants. The specificity of an aminotransferase from mung bean. Can J Biochem **43**: 723–730

Gil P, Dewey E, Friml J, Zhao Y, Snowden KC, Putterill J, Palme K, Estelle M, Chory J (2001) BIG: a calossin-like protein required for polar auxin transport in Arabidopsis. Genes Dev **15**: 1985–1997

Gray WM, Ostin A, Sandberg G, Romano CP, Estelle M (1998) High temperature promotes auxin-mediated hypocotyl elongation in Arabidopsis. Proc Natl Acad Sci USA **95**: 7197–7202

Grieneisen VA, Xu J, Maree AF, Hogeweg P, Scheres B (2007) Auxin transport is sufficient to generate a maximum and gradient guiding root growth. Nature **449**: 1008–1013

Harper RM, Stowe-Evans EL, Luesse DR, Muto H, Tatematsu K, Watahiki MK, Yamamoto K, Liscum E (2000) The NPH4 locus encodes the auxin response factor ARF7, a conditional regulator of differential growth in aerial *Arabidopsis* tissue. Plant Cell **12**: 757–770

Huelsenbeck JP, Ronquist F (2001) MRBAYES: Bayesian inference of phylogenetic trees. Bioinformatics **17**: 754–755

Hull AK, Vij R, Celenza JL (2000) Arabidopsis cytochrome P450s that catalyze the first step of tryptophan-dependent indole-3-acetic acid biosynthesis. Proc Natl Acad Sci USA **97**: 2379–2384

Kepinski S, Leyser O (2005) The Arabidopsis F-box protein TIR1 is an auxin receptor. Nature **435**: 446–451

Koga J (1995) Structure and function of indolepyruvate decarboxylase, a key enzyme in indole-3-acetic acid biosynthesis. Biochim Biophys Acta **1249**: 1–13

Kramer EM, Draye X, Bennett MJ (2008) Modelling root growth and development. SEB Exp Biol Ser **61**: 195–211

Kuettner EB, Hilgenfeld R, Weiss MS (2002) The active principle of garlic at atomic resolution. J Biol Chem **277**: 46402–46407

Lieberman M (1979) Biosynthesis and action of ethylene. Annu Rev Plant Physiol **30**: 533–591

Lincoln C, Britton JH, Estelle M (1990) Growth and development of the axr1 mutants of *Arabidopsis*. Plant Cell **2**: 1071–1080

Ljung K, Bhalerao RP, Sandberg G (2001) Sites and homeostatic control of auxin biosynthesis in Arabidopsis during vegetative growth. Plant J **28**: 465–474

Ljung K, Hull AK, Celenza J, Yamada M, Estelle M, Normanly J, Sandberg G (2005) Sites and regulation of auxin biosynthesis in *Arabidopsis* roots. Plant Cell **17**: 1090–1104

Luschnig C, Gaxiola RA, Grisafi P, Fink GR (1998) EIR1, a root-specific protein involved in auxin transport, is required for gravitropism in *Arabidopsis thaliana*. Genes Dev **12**: 2175–2187

Maddison DR, Maddison WP (2003) MacClade 4: Analysis of Phylogeny and Character Evolution. Sinauer Associates, Sunderland, MA

Marchant A, Kargul J, May ST, Muller P, Delbarre A, Perrot-Rechenmann C, Bennett MJ (1999) AUX1 regulates root gravitropism in Arabidopsis by facilitating auxin uptake within root apical tissues. EMBO J **18:** 2066–2073

Muller A, Guan C, Galweiler L, Tanzler P, Huijser P, Marchant A, Parry G, Bennett M, Wisman E, Palme K (1998) AtPIN2 defines a locus of Arabidopsis for root gravitropism control. EMBO J **17:** 6903–6911

Notredame C, Higgins DG, Heringa J (2000) T-Coffee: a novel method for fast and accurate multiple sequence alignment. J Mol Biol **302:** 205–217

Patten CL, Glick BR (1996) Bacterial biosynthesis of indole-3-acetic acid. Can J Microbiol **42:** 207–220

Petersson SV, Johansson AI, Kowalczyk M, Makoveychuk A, Wang JY, Moritz T, Grebe M, Benfey PN, Sandberg G, Ljung K (2009) An auxin gradient and maximum in the *Arabidopsis* root apex shown by high-resolution cell-specific analysis of IAA distribution and synthesis. Plant Cell **21:** 1659–1668

Quint M, Gray WM (2006) Auxin signaling. Curr Opin Plant Biol **9:** 448–453

Ruegger M, Dewey E, Gray WM, Hobbie L, Turner J, Estelle M (1998) The TIR1 protein of Arabidopsis functions in auxin response and is related to human SKP2 and yeast grr1p. Genes Dev **12:** 198–207

Ruegger M, Dewey E, Hobbie L, Brown D, Bernasconi P, Turner J, Muday G, Estelle M (1997) Reduced naphthylphthalamic acid binding in the tir3 mutant of *Arabidopsis* is associated with a reduction in polar auxin transport and diverse morphological defects. Plant Cell **9:** 745–757

Růžicka K, Ljung K, Vanneste S, Podhorská R, Beeckman T, Friml J, Benková E (2007) Ethylene regulates root growth through effects on auxin biosynthesis and transport-dependent auxin distribution. Plant Cell **19:** 2197–2212

Sabatini S, Heidstra R, Wildwater M, Scheres B (2003) SCARECROW is involved in positioning the stem cell niche in the Arabidopsis root meristem. Genes Dev **17:** 354–358

Scheres B (2007) Stem-cell niches: nursery rhymes across kingdoms. Nat Rev Mol Cell Biol **8:** 345–354

Sheldrake AR (1973) The production of hormones in higher plants. Biol Rev Camb Philos Soc **48:** 509–559

Spaepen S, Vanderleyden J, Remans R (2007) Indole-3-acetic acid in microbial and microorganism-plant signaling. FEMS Microbiol Rev **31:** 425–448

Stepanova AN, Hoyt JM, Hamilton AA, Alonso JM (2005) A Link between ethylene and auxin uncovered by the characterization of two root-specific ethylene-insensitive mutants in *Arabidopsis*. Plant Cell **17:** 2230–2242

Stepanova AN, Robertson-Hoyt J, Yun J, Benavente LM, Xie DY, Dolezal K, Schlereth A, Jurgens G, Alonso JM (2008) TAA1-mediated auxin biosynthesis is essential for hormone crosstalk and plant development. Cell **133:** 177–191

Swofford DL (1998) PAUP. Phylogenetic Analysis Using Parsimony (and Other Methods). Sinauer Associates, Sunderland, MA

Tam YY, Normanly J (1998) Determination of indole-3-pyruvic acid levels in Arabidopsis thaliana by gas chromatography-selected ion monitoring-mass spectrometry. J Chromatogr A **800:** 101–108

Tao Y, Ferrer JL, Ljung K, Pojer F, Hong F, Long JA, Li L, Moreno JE, Bowman ME, Ivans LJ, et al (2008) Rapid synthesis of auxin via a new tryptophan-dependent pathway is required for shade avoidance in plants. Cell **133:** 164–176

Truelsen TA (1973) Indole-3-pyruvic acid as an intermediate in the conversion of tryptophan to indole-3-acetic acid. II. Distribution of tryptophan transaminase activity in plants. Physiol Plant **28:** 67–70

Vieten A, Sauer M, Brewer PB, Friml J (2007) Molecular and cellular aspects of auxin-transport-mediated development. Trends Plant Sci **12:** 160–168

Woodward AW, Bartel B (2005) Auxin: regulation, action, and interaction. Ann Bot (Lond) **95:** 707–735

Zhao Y, Christensen SK, Fankhauser C, Cashman JR, Cohen JD, Weigel D, Chory J (2001) A role for flavin monooxygenase-like enzymes in auxin biosynthesis. Science **291:** 306–309

Zhao Y, Hull AK, Gupta NR, Goss KA, Alonso J, Ecker JR, Normanly J, Chory J, Celenza JL (2002) Trp-dependent auxin biosynthesis in Arabidopsis: involvement of cytochrome P450s CYP79B2 and CYP79B3. Genes Dev **16:** 3100–3112